JOURNAL OF CATALYSIS 149, 254–267 (1994)

Application of Isotopic Transient Kinetics to Vinyl Acetate Catalysis

E. A. Crathorne, D. MacGowan,[1] S. R. Morris, and A. P. Rawlinson

BP International Limited, Research and Engineering Centre, Chertsey Road, Sunbury-on-Thames, Middlesex TW16 7LN, United Kingdom

Received July 26, 1993; revised May 11, 1994

The isotopic transient kinetics technique has been used to characterise the surface species of Pd/Cd/silica and Pd/Au/silica catalysts for vinyl acetate synthesis. The main feature of both types of catalyst is a substantial film of acetic acid and water equivalent to between two and three molecular layers. Additional temperatureprogrammed desorption experiments have shown that the amount of retained acetic acid is increased by the presence of palladium and the potassium acetate promoter. No reversibly chemisorbed ethylene or oxygen was detected. The major by-product, CO_2, was derived equally from ethylene and acetic acid under these conditions. Analysis of the isotopic transients of the vinyl acetate product has allowed an estimate of the active site densities to be calculated. The transients also contain information about product diffusivity. © 1994 Academic Press, Inc.

1. INTRODUCTION

Vinyl acetate (VA) is an important chemical intermediate used in the manufacture of paints, surface coatings, and adhesives (1). It is currently produced by the gas-phase reaction of ethylene, acetic acid, and oxygen using a palladium-based catalyst:

$$C_2H_4 + CH_3COOH + \tfrac{1}{2}O_2 = CH_3COO \cdot C_2H_3 + H_2O.$$

Moiseev *et al.* reported the homogeneous conversion of ethylene and acetic acid to vinyl acetate in 1960 (2). This process employed the chlorides of palladium and copper with sodium acetate and was used commercially by several companies including ICI (3). Some years later, Bayer (4) and Hoechst (5) simultaneously developed similar gas-phase processes which employed heterogeneous, palladium-based catalysts. These proved to be attractive alternatives to the liquid-phase process, eliminating corrosion (by avoiding chloride components) and substantially reducing by-product formation.

Hoechst and Bayer catalysts differ in their components and methods of preparation. With Hoechst catalysts, the three components—palladium acetate, cadmium acetate, and potassium acetate—are impregnated evenly throughout the silica support (in the form of 5-mm spheres). The palladium acetate is reduced to palladium metal in a second stage (6). With the Bayer catalyst and the later version patented by Du Pont (7), palladium and gold are impregnated as their chloride salts and reduced to give a thin outer shell of metals around the spherical silica pellet. Potassium acetate is then impregnated uniformly throughout the catalyst.

In this work we have used the isotopic transient kinetics (ITK) technique to study various catalyst types at 401 kPa and 423–428 K. Temperature-programmed desorption (TPD) experiments have been carried out to examine acetic acid adsorption. Isotope labelling has also been used to determine the source of the major nonselective product, CO_2.

ITK is a powerful method for probing the basic kinetics of the important surface reactions of a chemical process (8). It involves an instantaneous switch between feeds of equal composition but different isotopic makeup. The steady-state reactions remain unperturbed but the imposed isotopic transient essentially titrates adsorbed surface species from the catalyst. Detailed information about the concentrations and lifetimes of the active species as well as kinetic data can be obtained by monitoring these processes.

The technique has been developed over a number of years primarily for the characterisation of Fischer–Tropsch catalysts [e.g. Ref. (9)], although other reaction processes have also been studied (10, 11). Generally, low-surface-area, model catalysts are used to limit diffusional effects since these mask the reaction kinetics. However, model systems are often far removed from "real" catalysis and the resulting kinetic analysis is of little use for commercial modelling purposes. An appraisal of reactant and product diffusion is essential in understanding the response of a catalyst.

In this work, the catalyst formulations closely mimic those of genuine commercial systems in terms of surface area, pore structure, and metal and promoter loadings.

[1] To whom all correspondence should be addressed.

0021-9517/94 $6.00

This has undoubtedly complicated the analysis but our subsequent treatment, we believe, allows us to deconvolute the reaction kinetics and diffusion effects.

2. METHODS

2.1. Catalysts

The catalysts for the ITK experiments were prepared according to the methods of Du Pont (7) and Hoechst (6). In both cases the support material was Sud Chemie KA160 silica (180 $m^2\ g^{-1}$) in the form of 5- to 6-mm-diameter spheres. The uniformly impregnated Pd/Cd/silica/K catalyst had nominal loadings of 2.1 wt.% Pd, 2.0 wt.% Cd, and 2.4 wt.% K. The shell-impregnated catalyst had overall loadings of 0.56 wt.% Pd, 0.25 wt.% Au, and 2.9 wt.% K, although the Pd and Au were concentrated in the outer 0.5 mm of the silica sphere.

For the TPD experiments, additional catalysts were prepared using Sud Chemie KA2 silica spheres (4–5 mm in diameter, 127 $m^2\ g^{-1}$). These were impregnated with the acetate salts of palladium, cadmium, and potassium according to the Hoechst procedure (6). GS 1541 silica spheres (KaliChemie, 3–4 mm in diameter, 290 $m^2\ g^{-1}$) were also used in these experiments.

2.2. Isotopic Transient Kinetics

Three types of experiments were carried out and these required different reactor configurations (Fig. 1). In the $^{12}C_2H_4/^{13}C_2H_4$ exchange experiments the system was set up as shown in Fig. 1a. The same configuration was used for oxygen switching experiments except that the normal ethylene and oxygen feeds were interchanged and 18-oxygen was used in place of 13-ethylene. In both cases the pressures of the two gas feeds were equalised using a needle valve and differential pressure transducer. Argon was bled into the original feed ($^{12}C_2H_4$ or $^{16}O_2$). The front section of the reactor tube was used to vaporise the acetic acid feed. The acetic acid used in these experiments had 2% water added to mimic plant conditions more closely.

In the experiments where [^{12}C-]acetic acid (99.7% pure, no added water) was exchanged with [^{13}C-]acetic acid (labelled in either the first or second carbon position) a separate vaporiser was necessary for each feed (Fig. 1b). These were included in the same furnace. The acetic acid feeds were purged from the vaporisers by argon and nitrogen, respectively. Switches in the feeds were achieved using a four-port Valco valve and the pressures equalised by connecting the off-stream vaporiser outlet to a reactor bypass. This was then reconnected downstream of the reactor and sampling point but upstream of the back-pressure regulator. The valve and all feed lines were heated to about 403 K.

The catalyst bed temperature was monitored by a thermocouple taped to the outside of the reactor tube (5-mm internal diameter). Gas volumes were adjusted to maintain a gas hourly space velocity of 3850 h^{-1} and a liquid hourly space velocity of 1.08 h^{-1}. Prior to starting the isotope switching experiments, baseline data on the effect of reactor pressure were obtained for both types of catalyst. Each pressure was maintained for 2 h to obtain an average of the space time yield (STY, $mg_{VA}\ cm_{cat}^{-3}\ h^{-1}$). Conversion levels of all reactants were restricted to below 5%.

Since both gas flows and pressures were limited by the quantity and pressure of the isotopic supplies (Isotec Limited), smaller catalyst volumes were used for the switching experiments. Catalyst volumes of 2 cm^3 were used for preliminary experiments to determine the effect of reaction pressure, catalyst volumes between 0.5 and 1.0 cm^3 being used in the isotope switch experiments. In most cases full catalyst pellets were used, but for experiments with powdered catalysts these were crushed and sieved to 0.5–1.0 mm.

The sampling capillary of the mass spectrometer (a VG Quadrupole Spectralab 200) was situated at the rear of the reactor. Typically, sampling of between three and eight masses was achieved at 0.3- to 0.5-s intervals. The raw data were stored within the operating computer and then translated to a spreadsheet for further analysis.

The calculation of surface concentrations broadly followed the method of Biloen *et al.* (8). Analysis of the transient decay curves is described in the Appendix.

2.3. Temperature-Programmed Desorption (TPD) Experiments

In the TPD experiments, 4-cm^3 samples were saturated in a 15% acetic acid (99.7% pure)/helium gas stream at 428 K and 915 kPa. The bed temperature was then raised at 10 K min^{-1} to 523 K. In some cases, a cooling cycle was also employed to readsorb acetic acid. Changes in the gas-phase acetic acid concentration (as monitored by a gas chromatograph and mass spectrometer) allowed the volume of acid evolved (or readsorbed) to be calculated.

2.4. Isotope Tracer Experiments

Conventional isotopic tracer experiments were performed to determine the extent of C_2H_4 and acetic acid combustion. These experiments required the use of a series of traps to remove acetic acid and vinyl acetate from the effluent stream because of their substantial contributions to m/z 44 and 45 in the mass spectrometric analysis. An ice bath was sufficient to remove acetic acid but was not capable of removing all the vinyl acetate from the gas stream. This was achieved using a further trap consisting of acetone and solid CO_2 maintained at 218 K. In combination, these traps (Fig. 1a) allowed experiments to be performed for up to 30 min before acid or acetate breakthrough occurred.

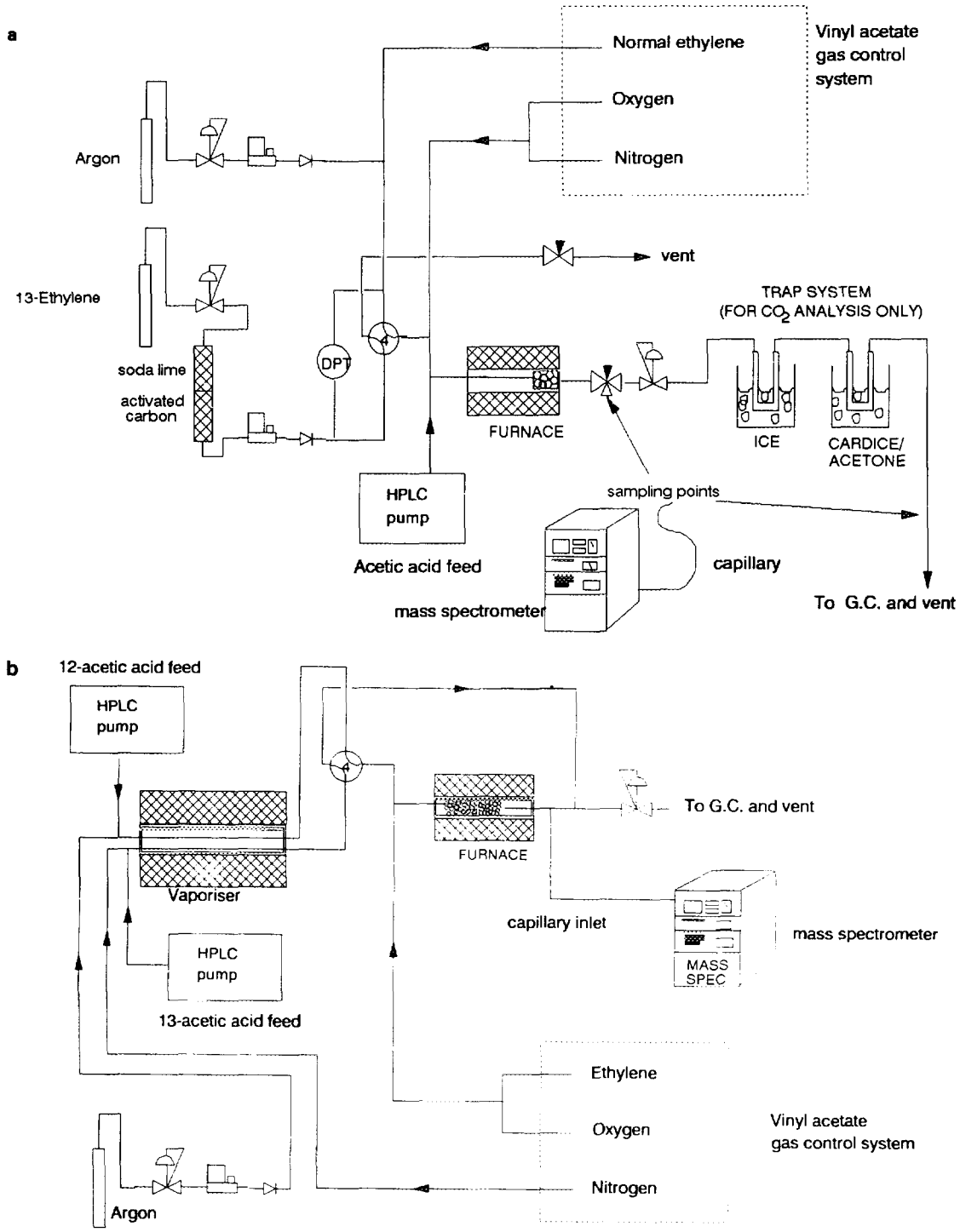

FIG. 1. (a) Apparatus used for ethylene (and oxygen) switching experiments. (b) Configuration for acetic acid exchange experiments.

An activated carbon trap was also needed to remove low levels of ethyl chloride and butenes from the $^{13}C_2H_4$ feed. Without this, catalyst deactivation was observed, although this was reversible and normal activity was resumed upon resumption of the $^{12}C_2H_4$ feed. Background measurements of m/z ratios 44 and 45 (in the $^{13}C_2H_4$ feed) were taken before and after each $^{13}C_2H_4$ switch. The $^{12}C_2H_4$, O_2, and N_2 feeds were used without further purification and the contribution of impurities to m/z 44 and 45 was subtracted during data analysis.

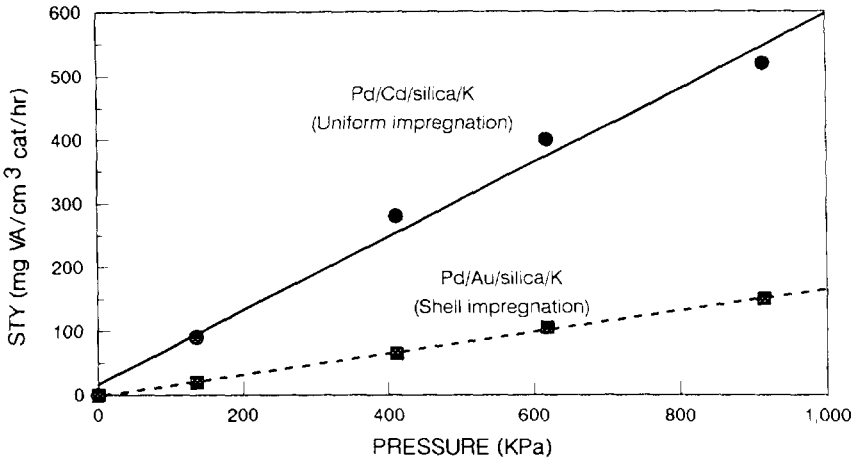

FIG. 2. Effect of total pressure on catalyst activity.

3. RESULTS

3.1. Catalyst Performance

The variation of catalyst activity and selectivity with reaction pressure was determined so that the results obtained in the isotope switch experiments at 401 kPa could be related to activity at normal reaction pressure (901 kPa). The results are shown in Fig. 2.

Activity was found to vary almost linearly with pressure. Selectivity toward vinyl acetate was found to depend on both pressure and time on stream. For the Pd/Cd/silica/K catalyst, for example, the VA : CO_2 molar ratio at 401–901 kPa was 7 : 1 during the period 2 to 6 h on stream and 10 : 1 after 21 to 26 h. At 136 kPa the selectivity was lower, with a VA : CO_2 ratio of 5 : 1.

3.2. Ethylene Exchange Experiments

The transient in unreacted ethylene following a $^{12}C_2H_4$/$^{13}C_2H_4$ switch is shown in Fig. 3. Within experimental error the argon and $^{12}C_2H_4$ decay curves are identical and superimposed. The level of reversibly adsorbed ethylene is therefore below the detection limit of the experiment (1 μmol g^{-1}).

The transients in the vinyl acetate product from samples of a fresh Pd/Cd/silica/K catalyst at 428 K and 401 kPa are shown in Fig. 4. Experiments were conducted on both whole and crushed pellets. Whilst the overall productivities of these samples were similar, the transients are clearly very different, suggesting variations in both the concentration and lifetime of vinyl acetate species. Since the decays of argon were identical the observed differences cannot be due to experimental variations.

It is unlikely that the simple act of crushing the catalyst pellets has changed the fundamental steps of the reaction or the active site concentration. We must therefore conclude that the desorption and elution of vinyl acetate are hindered in the pelleted sample. The majority of the vinyl acetate measured on this sample represents the quantity of vinyl acetate diffusing through the catalyst since this process is substantially slower than the rate of reaction. With the crushed catalyst, the lifetime of vinyl acetate in the system is shorter and close to the experimental limit of measurement. The number of species residing on the catalyst is also less (1.3 as opposed to 8.6 μmol g^{-1}) and is perhaps closer to a meaningful measure of the number of active sites.

With fresh Pd/Au/silica/K catalyst pellets the effects of diffusion are not observed to the same extent (Fig. 4). The Pd/Au/silica/K sample also contains fewer vinyl acetate species (0.9 μmol g^{-1}), which probably reflects the difference in active site concentration on the two catalysts.

A detailed analysis of the decay curves is discussed in Section 4.

3.3. Oxygen Exchange Experiments

No detectable transients or chromatographic delays were observed in the unreacted oxygen nor was any $^{16}O^{18}O$ observed. Any levels of reversibly chemisorbed oxygen are therefore below the level of detection for these experiments.

Within product water, oxygen exchange occurs over a period of about 15 min following a switch to $^{18}O_2$. This implies that a large reservoir of water is present on the catalyst during reaction (150–250 μmol g^{-1}). The isotopic exchange of oxygen into product CO_2 occurs on a similar time scale. However, full exchange is never achieved. Even after 20 min, when the pool of water is effectively

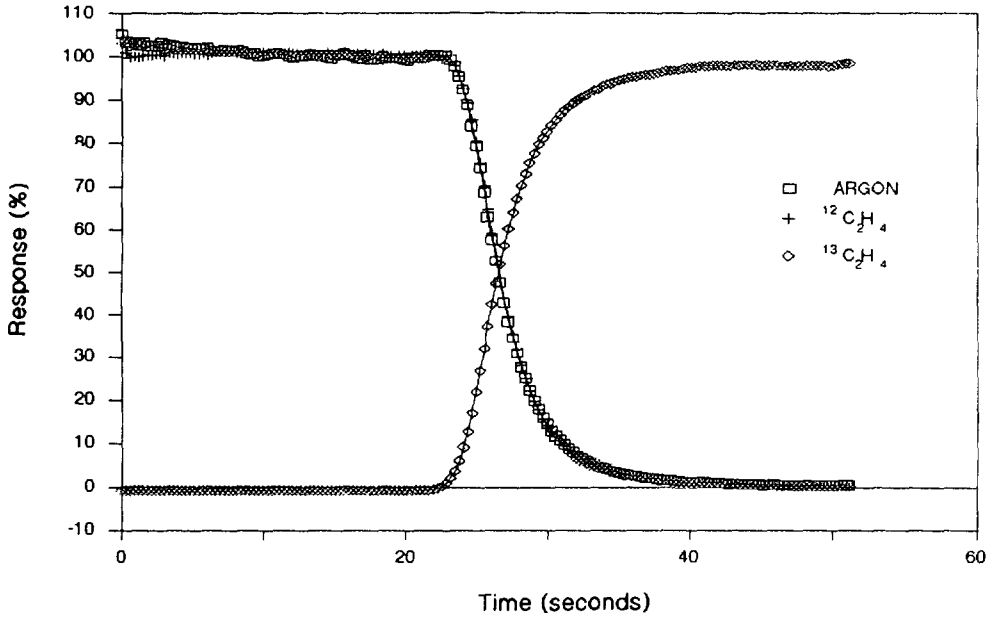

FIG. 3. Transient in unreached ethylene following $^{12}C_2H_4/^{13}C_2H_4$ switch over powdered Pd/Cd/silica/K catalyst.

all $H_2{}^{18}O$, CO_2 still contains a substantial fraction of ^{16}O. This suggests that a substantial proportion of the CO_2 originates from acetic acid (or vinyl acetate) oxidation. Quantification of these effects proved to be difficult. A more accurate method of assessing the relative oxidations of ethylene, acetic acid and vinyl acetate is discussed in Section 3.6.

3.4. Acetic Acid Exchange

An acetic acid exchange experiment over a Pd/Cd/silica/K catalyst is shown in Fig. 5. The acetic acid pool is large (1800 μmol g^{-1}) and nearly 3 min of feed was required to provide sufficient material for the exchange. No kinetics could therefore be obtained from the acid transient. Inclusion of ^{13}C from the acetic acid

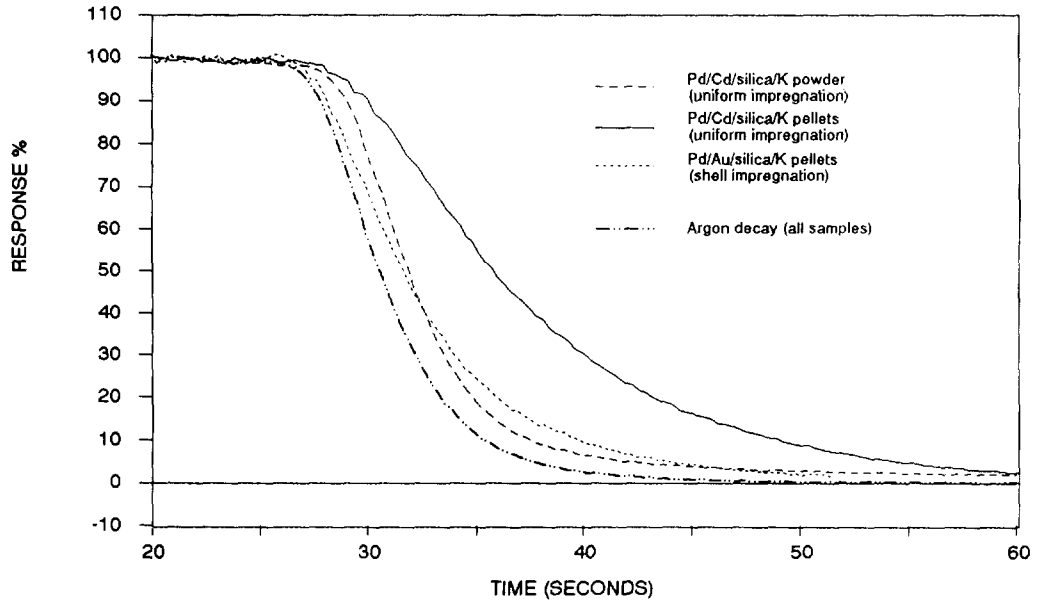

FIG. 4. Transient decay of [^{12}C]vinyl acetate following $^{12}C_2H_4/^{13}C_2H_4$ switch over fresh catalysts.

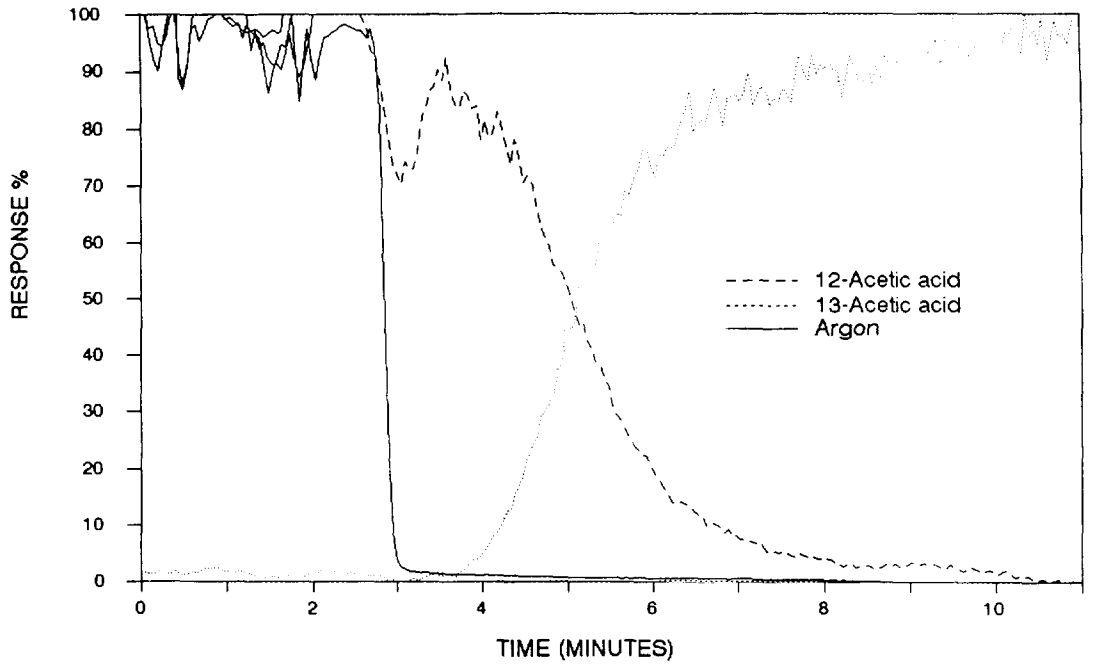

FIG. 5. $CH_3{}^{12}COOH/CH_3{}^{13}COOH$ exchange: response of unreacted acetic acid for Pd/Cd/silica/K pellets.

pool into the vinyl acetate product was also observed. A similar amount of acetic acid (1911 μmol g^{-1}) was found to be adsorbed on the Pd/Au/silica/K catalyst.

3.5 Temperature-Programmed Desorption Experiments

Acetic acid retention was measured on a range of model systems under normal operating conditions by a temperature-programmed desorption technique. It was found that acetic acid retention was sensitive not only to the surface area of the support but also to the loadings of potassium acetate and palladium (Table 1).

The amount of retained acetic acid increased with the surface area of the silica from 422 μmol g^{-1} on KA-2 (127 m^2 g^{-1}) to 699 μmol g^{-1} on GS 1541 (290 m^2 g^{-1}). With a 2.4 wt% loading of palladium (225 μmol g^{-1}) the amount of acid retained by the silica support increased from 422 to 600 μmol g^{-1}. Similarly, a 1.9 wt% potassium loading (487 μmol g^{-1}) increased the acid content to 801 μmol g^{-1}. The effects also seemed to be accumulative, with the acetic acid level increasing to 948 μmol g^{-1} on a sample containing the same loadings of both potassium and palladium. Cadmium acetate did not significantly affect acid retention.

TABLE 1

Acid Adsorption and the Influence of Catalyst Components

Loading (wt%)[a]			CH_3COOH adsorbed (μmol g^{-1})
Pd	Cd	K	
—	—	—	422
2.4	—	—	600
—	1.9	—	385
—	—	1.9	801
—	1.9	1.9	733
2.4	1.9	1.9	948

[a] Carrier used was Sud Chemie KA2 silica.

This TPD technique has since been shown to underestimate the levels of retained acetic acid by up to 60% because a significant fraction remains adsorbed at 523 K, the upper temperature of the temperature programme. Higher temperatures could not be used because of acid decomposition. However, the trends observed are probably still valid. The size of the acid film is clearly a complex function of silica surface area and the loadings of potassium and palladium.

3.6. Ethylene Tracer Experiments

For these experiments acetic acid and vinyl acetate were removed from the gas stream prior to mass spectrometric analysis. This was achieved using a combination of ice and cardice/acetone traps. The remaining gas stream then consisted solely of ethylene, oxygen, nitrogen, and carbon dioxide. The background levels of m/z 44 and 45 changed in a complicated fashion after the feed switch and increased as the traps became less efficient.

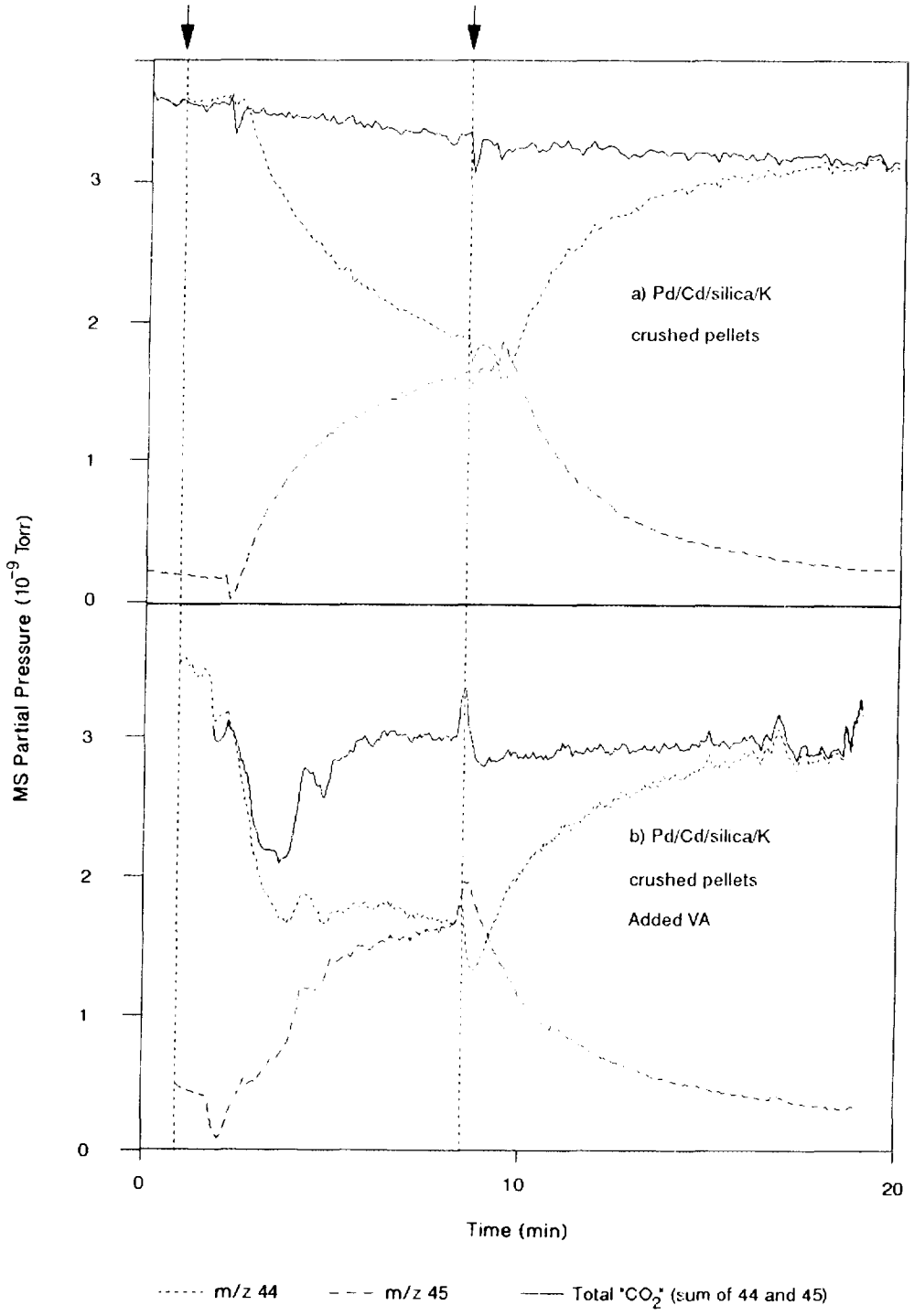

FIG. 6. Isotopic composition of CO_2 by-product during an extended period of $^{13}C_2H_4$ + $^{12}CH_3{}^{12}COOH$ feed. The first arrow indicates the switch to $^{13}C_2H_4$, and the second, the switch back to $^{12}C_2H_4$.

These were measured before and after each experiment and a background profile was simulated and subtracted from the data. For a crushed Pd/Cd/silica/K catalyst with a $^{13}C_2H_4$ feed (Fig. 6a), the equilibrium ratio of $^{12}CO_2$ to $^{13}CO_2$ was roughly 1 : 1.

A further experiment was carried out using the crushed Pd/Cd/silica/K sample. Vinyl acetate (wholly ^{12}C) was added to the acetic acid feed over the catalyst. The ethylene feed was then changed from $^{12}C_2H_4$ to $^{13}C_2H_4$ and the product CO_2 was monitored (Fig. 6b) and compared with

TABLE 2

Inventory of Surface Species on Working VA Catalysts

Surface species	Concentration (μmol g^{-1})[a] Pd/Cd/silica/K (uniform impregnation)	Pd/Au/silica/K (shell impregnation)
C_2H_4	<1.0	<1.0
O_2	<1.3	<2.6
VA	1.3	0.9
H_2O	154	230
AcOH	1800	1911

[a] Detection limits are related to gas-phase concentrations. For the reactants C_2H_4, O_2, and AcOH, the limits are roughly ± 1 μmol g^{-1}. For VA, present in substantially lower concentration, the sensitivity is correspondingly higher, approximately ± 0.1 μmol g^{-1}.

the experiment mentioned previously (Fig. 6a). The $^{12}CO_2/^{13}CO_2$ ratio appeared to be unaffected by the presence of additional vinyl acetate and remained approximately unity.

4. DISCUSSION

4.1. Kinetic Analysis

The full suite of isotopic transient experiments has permitted a detailed assessment of the surface species present on a vinyl acetate catalyst during reaction. These are summarised in Table 2. It was not possible to quantify the number and reactivity of the CO_2 species although some information has been obtained about the source of the nonselective product (see Section 4.2.2).

At 401 kPa and 428 K the predominant species on a working catalyst is acetic acid. The Pd/Cd/silica/K catalyst, for example, retains 1800 μmol g^{-1}. This agrees well with the figure of 1200 μmol g^{-1} which was recently reported for a Hoechst-type catalyst at 400–440 K/701 kPa as measured by a sorption method (12). Since the catalyst contains only 198 and 615 μmol g^{-1} palladium and potassium the majority of the acid must be associated with the silica support. The TPD results also indicate that the major factor in acid retention is the silica support, with secondary roles being played by the potassium acetate and palladium.

The distribution of the acid is unknown. A crude estimate, based on spheres packed to give the liquid density 0.89 g cm^{-3}, yields an acetic acid "footprint" of about 0.25 nm^2. For the pure silicas this gives a coverage less than a monolayer. However, the TPD results are believed to give an underestimate of the adsorbed acid. For the two catalyst types, which had surface areas in the range 90–100 m^2 g^{-1}, the acetic acid coverage is equivalent to about three molecular layers but the acid may not be evenly distributed over the silica surface. It could be associated with the potassium acetate promoter, with the metal centers, or with particular parts of the silica pore structure.

The ITK measurement of vinyl acetate species not only gives information about the active centers but also provides a means of calculating product diffusion rates. Since all the vinyl acetate is produced within the catalyst pore structure it provides an ideal probe of the local environment.

A simple way of using the theory in the Appendix to extract physical coefficients is to use Eq. (A14) to fit the 12-VA response for Pd/Cd/silica/K pellets. The resultant fit is shown in Fig. 7 and yields the values $\alpha = 0.500$ s^{-1}, $\beta = 0.457$ s^{-1}, and $\gamma_1 = 0.112$ s^{-1}, where α is the specific rate of VA formation and β accounts for the effects of voidage and γ_1 for pore transport. The steady-state response X^* and the time t_0 of the isotope switch are also included as fitting parameters. t_0 in particular is difficult to access more directly due to the smooth turnover of the response function. The value of β should also be obtainable via Eq. (A3) from the decay rate of argon (Fig. 8). The result from this is $\beta = 0.460$ s^{-1}, close to the value deduced from the 12-VA response. The consistency of the two β values supports the correctness of the theory.

Taking the Pd/Cd/silica/K pellet diameter to be 5.5 mm, it can be estimated from γ_1 that the effective diffusivity D of VA in the catalyst is 8.6×10^{-4} cm^2 s^{-1}. For the powdered Pd/Cd/silica/K, particle size is decreased by at least a factor of 5, and so γ_1 is increased by a factor of at least 25, relative to pellets. Therefore 12-VA loss

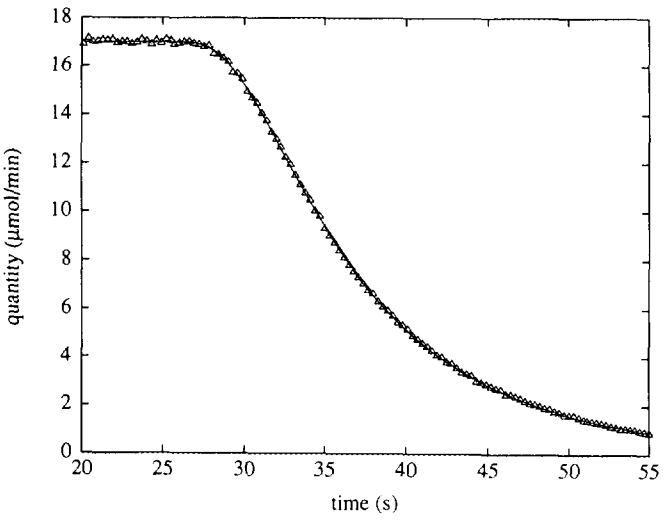

FIG. 7. [^{12}C]Vinyl acetate decay for Pd/Cd/silica/K pellets. Symbols: experiment; line: theoretical fit with parameters $X^* = 17.0$ μmol min^{-1}, $t_0 = 25.9$ s, $\alpha = 0.500$ s^{-1}, $\beta = 0.457$ s^{-1}, and $\gamma_1 = 0.112$ s^{-1}.

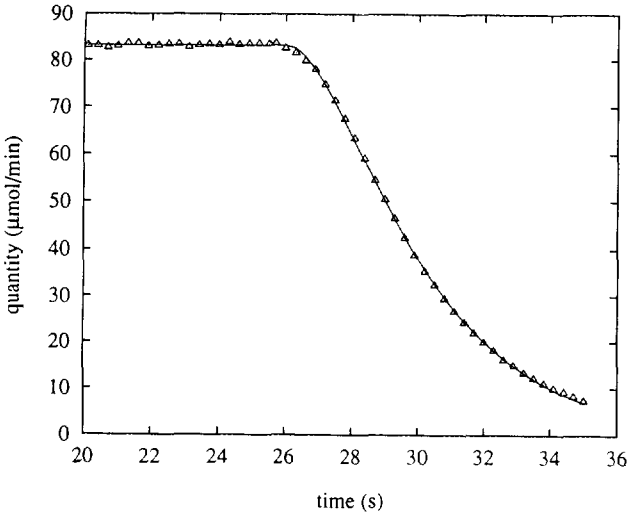

FIG. 8. Argon decay for Pd/Cd/silica/K powder. Symbols: experiment; line: theoretical fit with parameters $X^* = 83.2$ μmol min^{-1}, $t_0 = 26.0$ s, and $\beta = 0.460$ s^{-1}.

from the powder should be dominated by α and β except at short times. Fitting these data with Eq. (A14) gives very satisfactory visual agreement but the choice of an optimum value of γ_1 is difficult. This may be due to the range of sizes and shapes present in the powder. Assuming $\gamma_1 \rightarrow \infty$, an unambiguous fit is obtained with $\alpha = 1.08$ s^{-1}, $\beta = 0.455$ s^{-1} (Fig. 9). Whilst the β values obtained from the different fits are all consistent, values of α differing by a factor 2 are found for pellets and powder. It is difficult to be sure of the reason for this. It could be caused by the range of shapes and sizes in the powder (when pellet data should give the correct value), by an inability to distinguish more than the smallest two exponents for the pellets (when powder data should give the correct value), or by a deficiency of the theoretical approach to the voids.

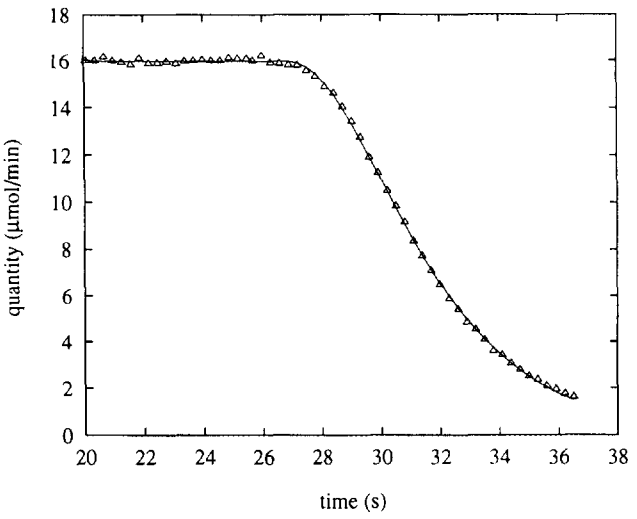

FIG. 9. [^{12}C]Vinyl acetate decay for Pd/Cd/silica/K powder. Symbols: experiment; line: theoretical fit with parameters $X^* = 16.0$ μmol min^{-1}, $t_0 = 26.6$ s, $\alpha = 1.08$ s^{-1}, and $\beta = 0.455$ s^{-1}.

4.2. Mechanistic Implications

4.2.1. Vinyl acetate formation. Two mechanistic schemes have been proposed for gas-phase, palladium-catalysed, VA synthesis. One, suggested by Nakamura and Yasui (13, 14), assumes the palladium remains in metallic form throughout the reaction, the feed components being adsorbed on the palladium surface. Coordinated acetate then reacts with a vinyl palladium species to give vinyl acetate:

$$C_2H_4 + 2Pd = CH_2\text{–}CH\text{–}Pd + PdH$$
$$O_2 + 2Pd = 2Pd\text{–}O$$
$$CH_3COOH + Pd = Pd \cdot CH_3COOH$$
$$PdCH_3COOH + PdO = Pd\text{–}OCOCH_3 + Pd\text{–}OH$$
$$PdOCOCH_3 + CH_3CHPd = PdCH_2CHOCOCH_3 + Pd$$
$$PdCH_2CHOCOCH_3 = VA + Pd$$
$$Pd\text{–}OH + Pd\text{–}H = PdH_2O + Pd$$

The second mechanism, proposed by Zaidi (15) and Samanos *et al.* (16), assumes that the reaction occurs in a manner similar to that of the homogeneous system (17). In this, coordinated ethylene inserts into one of the Pd–OAc bonds of a palladium/alkali metal acetate complex which then decomposes to give vinyl acetate and palladium metal. An oxidant such as quinone or Cu^{2+} is generally used to reoxidise the palladium to palladium acetate (18). The reoxidation can occur in air but, in solution, the rate of dissolution is low (19). In the proposed heterogeneous analogue of this reaction some of the palladium is oxidised to palladium acetate. The kinetic limitations of this reaction may be alleviated since the palladium is highly dispersed:

$$Pd + \tfrac{1}{2}O_2 + 2AcOH = Pd(OAc)_2 + H_2O$$
$$Pd(OAc)_2 + AcO^- = Pd(OAc)_3^-$$

This species then reacts with C_2H_4 from the gas phase, giving vinyl acetate and regenerated palladium metal:

$$Pd(OAc)_3^- + C_2H_4 = VA + AcOH + AcO^- + Pd$$

Under working conditions both catalyst types possess a high concentration of adsorbed acetic acid equivalent to three molecular layers. This is clearly insufficient even

to provide a full coordination sphere and should not therefore be thought of as a true liquid. Nevertheless, this film must play a significant role since many features of the catalysts maximise retention (potassium acetate, support pore structure). The TPD results show that some adsorption of acetic acid on palladium metal occurs under reaction conditions but adsorption of acid on the silica surface and by the potassium acetate could also be important.

The number of vinyl acetate precursors (or active sites) accounted for only about 2% (Du Pont-type catalyst) and 0.7% (Hoechst-type catalyst) of the total palladium metal loading. This assumes a one-to-one relationship between vinyl acetate and palladium at each active site. No reversible ethylene or oxygen adsorption was observed (although the sensitivity of these experiments was not as high as for VA measurements). If adsorbed ethylene and/or oxygen are important during the catalysis then the number of adsorbing sites is exceptionally low (<1 μmol g^{-1}) when compared with the amount of acid and water. These observations are compatible with a supported liquid-phase reaction scheme.

4.2.2. Carbon dioxide formation. Under normal plant conditions VA catalysts operate with a selectivity well in excess of 90%. The major by-product is CO_2 and this could originate from full oxidation of either of the hydrocarbon feeds or the vinyl acetate product. The relative importance of these various oxidations is rather difficult to determine and views within the open literature are conflicting. Various authors have assumed that ethylene oxidation predominates, although this is based on the observation that the rates of the individual oxidations follow the order $C_2H_4 > VA > CH_3COOH$. In the only isotopic labelling experiments aimed at determining the source of CO_2, acetic acid oxidation dominated at reduced pressure (20).

Our isotope tracer experiments indicate that the ratio of ethylene and acetic acid oxidations over a Pd/Cd/silica/K catalyst at 423 K and 401 kPa was roughly 1 : 1. When [^{12}C-]vinyl acetate was added to the feed the proportion of $^{12}CO_2$ was not increased. This shows that the secondary combustion of vinyl acetate is not significant. However, this observation does not totally rule out vinyl acetate oxidation as a source of CO_2. Gas-phase vinyl acetate may not chemisorb or interact strongly with the catalyst although the active intermediate itself may be prone to combustion. It would be difficult experimentally to discriminate between the individual or intermediate routes to CO_2 formation. Simply by studying catalysts under different conditions the isotopic ratio may be observed to vary from unity, thereby implicating the oxidation of the individual reactants. Even so, the oxidation of the active intermediate could not be entirely ruled out unless product CO_2 consisted of only one isotopic composition. Further experiments are required to clarify this.

5. CONCLUSIONS

Vinyl acetate synthesis has provided a challenging system for study by transient kinetics. Our results highlight the complexities of the reaction, with the major feature being the presence of a substantial, condensed film of acetic acid and water. TPD experiments show that acetic acid retention is a complex function of surface area and potassium acetate and palladium loadings. No reversibly chemisorbed oxygen or ethylene was detected. These findings are consistent with a supported liquid-phase type of mechanism. Isotope analysis of the nonselective product CO_2 has shown that it is derived equally from both ethylene and acetic acid at 423 K and 401 kPa.

The transient in product vinyl acetate was determined primarily by diffusion effects for uniformly impregnated catalyst pellets. For crushed pellets or shell-impregnated catalysts these effects are reduced. A detailed analysis of the transient decays has been developed to deconvolute the effects of product formation and gas transport in both voids and pores.

Through the isotopic transient kinetics technique, detailed kinetic descriptions have been provided for systems of commercial significance. With these results (active site estimates, surface concentrations, specific rates, transport characteristics) it becomes possible to construct a truly predictive, mechanistically based reactor model.

APPENDIX: REACTION-DIFFUSION ANALYSIS

The Appendix attempts to interpret ethylene isotope switch results using solutions of macroscopic reaction-diffusion equations. It is assumed that steady-state operation has been achieved prior to the isotope switch (at time $t = 0$) and that the pellet surface acts as an absorbing boundary for VA (i.e., as soon as a VA molecule reaches the surface it is rapidly removed into a fast-flowing product stream). Throughout the analysis steady-state (pre-switch) values are denoted by an asterisk.

It is convenient to define the functions $e_n(t|\mathbf{v})$ for positive integers n by

$$e_n(t|\mathbf{v}) = 1, \qquad t \le 0,$$

$$e_n(t|\mathbf{v}) = \sum_{i=1}^{n} \frac{\exp(-v_i t)}{\prod_{j \neq i}(1 - v_i/v_j)}, \qquad t \ge 0,$$

where $\mathbf{v} = (v_1, v_2, \ldots, v_n)$. All the results of the analysis below can be expressed in terms of the e_n. Note that $e_1(t|\mathbf{v})$ is just a single exponential for $t \ge 0$ and so e_1 has a discontinuity in its derivative at $t = 0$. As n increases from 1, successively higher derivatives of e_n vanish for $t \to 0+$. It has been implicitly assumed above that all v_i are distinct. Singular cases with two or more v_i identical

are easily dealt with by treating the equal exponents as distinct and considering the appropriate limit. Indeed when some of the v_i are close but not identical, the evaluation of e_n is done by series expansion to minimise numerical error.

Transport Outside the Pellets

The experimental results cannot be fully interpreted in terms of transport in the pellets alone, because gases must pass through the voids of the microreactor to be detected. To quantify this transport in voids, consider the significance of the use of argon, which is added to the $^{12}C_2H_4$ but not the $^{13}C_2H_4$ in the transient kinetics experiments. Argon is very sparingly soluble in the acetic acid layers in the catalyst pores and therefore suffers no significant diffusional resistance. Experimental evidence for this assertion comes from Fig. 4, where it can be seen that the loss of argon from the microreactor is independent of whether the catalyst is in pellets or crushed.

Let $\sigma_P(t)$ and $\sigma_V(t)$ denote the densities of argon in the pellets and voids of the microreactor respectively at time t. These are spatially averaged densities in contrast to the local densities within the pellets introduced below. The argon transfer between the pellets and voids is described by the phenomenological mass transfer equation

$$d\sigma_V/dt = -\beta(\sigma_V - \sigma_P/\phi) \qquad \text{(A1)}$$

with transfer coefficient β. In the steady state, $\sigma_P^* = \phi\sigma_V^*$ and so ϕ is simply related to the Henry constant. ϕ should be close to the vapour-filled porosity of the pellet (excluding volume occupied by liquid acetic acid layers) so that the local argon density in the pores of the pellets will be close to that in the voids.

The solution of Eq. (A1) is

$$\sigma_V = \sigma_V^* \exp(-\beta t) + (\beta/\phi)\int_0^t ds\, \sigma_P(s) \exp\{-\beta(t-s)\}. \qquad \text{(A2)}$$

To obtain an explicit result for σ_V, an expression must be obtained for $\sigma_P(t)$. Consider diffusion of argon (effective diffusivity D_A) in a spherical catalyst pellet of radius a. Provided that attention is restricted to times such that $D_A t/a^2 \gg 1$, diffusional resistance to argon can be ignored and argon density in the pellet remains spatially uniform ($= \sigma_P$) at all times. The time dependence is taken to be $\sigma_P = \sigma_P^* e_1(t|\beta)$, representing instantaneous Henry's law equilibrium between the pellet and the void. Note, however, the exclusion from the void density *for purposes of determining* σ_P of argon that was originally in a pellet at the switch time, represented by the convolution term in Eq. (A2). This is consistent with the use of the absorbing boundary condition for 12-VA alluded to above and implemented below, since no 12-VA originates outside the pellets. The explicit form of Eq. (A2) for this σ_P is

$$\sigma_V/\sigma_V^* = e_2(t|\beta,\beta) = (1+\beta t)\exp(-\beta t). \qquad \text{(A3)}$$

The final expression in (A3) is valid only for $t \geq 0$.

Equations similar to (A1) and (A2) are also used to describe the transient kinetics of 12-VA but, because it is a reaction product, it is best described using quantities rather than densities. Let $N_V(t)$ denote the quantity of 12-VA in the voids and $n_P(t)$ the rate of 12-VA loss from the pellets to the voids, both at time t. Then

$$dN_V/dt = -\beta N_V + n_P. \qquad \text{(A4)}$$

The same parameter β is used for both species. In doing this, it is assumed that the loss of each gas from the voids is proportional to the quantity of that gas present in the voids, the proportionality constant being species independent. Clearly the steady-state condition for 12-VA is $n_P^* = \beta N_V^*$ and the solution of (A4) is

$$N_V = N_V^* \exp(-\beta t) + \int_0^t ds n_P(s) \exp\{-\beta(t-s)\}. \qquad \text{(A5)}$$

The convolution form of the last term clearly implies the assumption that, once a molecule escapes from a pellet, it behaves on average like the VA molecules in the void at the switch time: in particular there are no stagnant boundary layers near the pellets. It would be difficult to analyse the effect of the transport in voids on the experimental data without making some such assumption.

The quantities of argon and 12-VA measured by transient kinetics are proportional to $\sigma_V(t)$ and $N_V(t)$, respectively. It might be thought that rates are being measured, especially since the experimental data are quantities per minute. However, it is clear that the mass spectrometer samples the composition; the rate aspect of the experimental data is associated with pumping gas into the spectrometer.

12-VA Production and Diffusion in a Pellet

Consider a spherical shell-impregnated catalyst pellet of radius a. Active sites are confined to an outer shell $b < r < a$ and it will be assumed that they are distributed uniformly within this shell. A uniformly impregnated catalyst can be regarded as the special case $b = 0$ and is in that sense also covered by the following analysis. VA production is believed to take place by a two-stage mechanism: relatively rapid formation of an intermediate from which VA forms more slowly. Since plentiful acetic acid is available at active sites and other reactants reach them

easily by rapid diffusion, the rate of intermediate production per active site can reasonably be assumed independent of the position of the active site within a catalyst pellet and proportional to the local ethylene concentration.

It is advantageous to begin by writing down equations for the densities of all entities that can incorporate $^{12}C_2H_4$—$^{12}C_2H_4$ itself (ρ_E), 12-intermediates (ρ_I), and 12-VA product (ρ):

$$\partial\rho_E/\partial t = D_E\nabla^2\rho_E - \mu\rho_E, \quad b < r < a, \tag{A6}$$

$$d\rho_I/dt = \mu\rho_E - \alpha\rho_I, \quad b < r < a, \tag{A7}$$

$$\partial\rho/\partial t = D\nabla^2\rho + \alpha\rho_I, \quad b < r < a. \tag{A8}$$

Here D_E and D are the effective diffusivities of ethylene and VA, respectively, $\mu\rho_E$ is the rate of production of intermediates from reactants, and $\alpha\rho_I$ is the rate of product formation from intermediates (both per unit volume). It is assumed that diffusivities are the same for the shell and the interior. This appears reasonable since there is no significant difference in pore structure caused by metal impregnation of the catalyst support. In writing (A7) it is also assumed that the intermediates are immobile. For $0 < r < b$, $\rho_I = 0$ and $\alpha = \mu = 0$ so that Eqs. (A6) and (A8) reduce to simple diffusion equations. From Fig. 3, it can be seen that the ethylene decay is the same as that for argon, providing experimental evidence that formation of intermediates from ethylene suffers no diffusion limitation (i.e., $\mu a^2/D_E \ll 1$). The last term in Eq. (A6) can therefore be neglected and the equation

$$\partial\rho_E/\partial t = D_E\nabla^2\rho_E \tag{A9}$$

replaces (A6).

The steady-state solution of Eqs. (A7)–(A9) must first be sought by setting all time derivatives to zero. The appropriate boundary conditions for $\rho_E^*(r)$ are $\rho_E^*(a) = R$, where R is some constant related to a Henry constant and the density of ethylene in the voids, and $\rho_E^*(0)$ finite. Solving (A9), $\rho_E^*(r) = R$ for all $r < a$. Consequently, $\rho_I^*(r) = S \equiv \mu R/\alpha$ for $b < r < a$. Equation (A8) can now be solved with boundary conditions $\rho^*(a) = 0$, $\rho^*(0)$ finite, and continuity of ρ^* and $d\rho^*/dr$ at $r = b$, to give

$$\rho^*(r) = [\alpha S/(6D)]\,[a^2 + 2b^3a^{-1} - 3b^2], \quad 0 < r < b,$$

$$\rho^*(r) = [\alpha S/(6D)]\,[a^2 - r^2 + 2b^3(a^{-1} - r^{-1})], \quad b < r < a. \tag{A10}$$

Turning to the transients after the switch, the full time-dependent form of Eqs. (A7)–(A9) must be solved with initial conditions given by the steady-state solutions. For consistency with the treatment of gas in the voids (see calculation for argon), the outer boundary condition for ethylene is taken as $\rho_E(a, t) = R\exp(-\beta t)$. Boundary conditions for $\rho(r, t)$ are the same as for the corresponding steady-state solution. In view of the lack of diffusional resistance for ethylene, $\rho_E(r, t)$ remains spatially uniform for $t > 0$, so that ρ_I stays uniform over the active shell:

$$\rho_I(r, t) = Se_2(t|\alpha, \beta), \quad b < r < a. \tag{A11}$$

The solution of Eq. (A8) with its associated conditions can now be obtained by eigenfunction expansion. Integrating the resultant $\rho(r, t)$ over the sphere volume gives $N_P(t)$, the total amount of 12-VA in the pellet at time t. $n_P(t)$, the rate of 12-VA loss from the pellet at time t, may be calculated from a simple mass balance taking into account the delayed 12-VA production,

$$n_P(t) = -dN_P/dt + 4\pi\alpha\int_0^a \rho_I(r, t)r^2\,dr.$$

The result for 12-VA loss from a pellet can be written as

$$n_P(t)/n_P^* = F\Sigma G_k e_3(t|\alpha, \beta, \gamma_k) \tag{A13}$$

where $G_k = [k\pi - k\pi(1 - \varepsilon)\cos(k\pi\varepsilon) - \sin(k\pi\varepsilon)]/(k\pi)^3$; $\varepsilon = (a - b)/a$ is the shell thickness as a fraction of pellet radius, $\gamma_k = k^2\pi^2D/a^2$; and $F = 6/[\varepsilon(3 - 3\varepsilon + \varepsilon^2)]$. The denominator of F is the ratio of active shell volume to spherical pellet volume.

Finally, the 12-VA transient kinetics response can be obtained from Eqs. (A5) and (A13):

$$Z(t) \equiv N_V(t)/N_V^* = F\Sigma G_k e_4(t|\alpha, \beta, \beta, \gamma_k). \tag{A14}$$

The summations above extend over all positive integers k. Results for a uniformly impregnated catalyst are easily obtained by setting $\varepsilon = 1$ [$F = 6$, $G_k = 1/(k\pi)^2$].

Note that $[dn_P/dt]_{t=0} = [d^2n_P/dt^2]_{t=0} = 0$ so that $n_P(t)$, has its first two derivatives continuous and cubic behaviour at short times after the switch. On the other hand, $[dN_V/dt]_{t=0} = [d^2N_V/dt^2]_{t=0} = [d^3N_V/dt^3]_{t=0} = 0$ so that $N_V(t)$ has its first three derivatives continuous and quartic behaviour at short times after the switch. This may be contrasted with the loss of argon (or ethylene) from the microreactor which can be seen from Eq. (A3) to be quadratic shortly after the switch. It is also interesting that relative volumes of pellets and voids do not appear in the final results because the use of the mass balances in the steady state implicitly incorporates such factors.

Some examples of $N_V(t)/N_V^*$ plotted semilogarithmic-

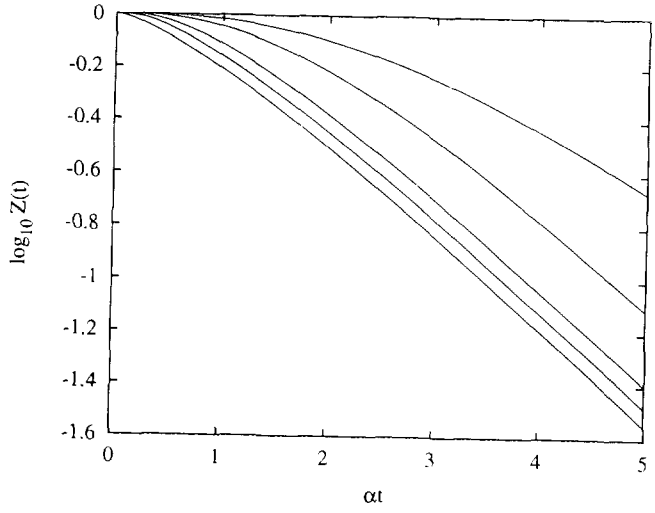

FIG. A1. β dependence of $Z(t)$ [Eq. (A14)] for $\gamma_1 = \alpha$, $\varepsilon = 1$. Curves from top: $\beta/\alpha = 1, 2, 5, 10, 100$.

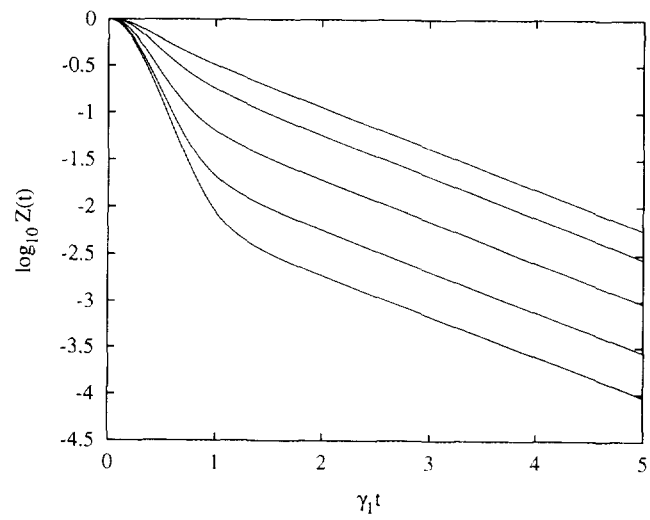

FIG. A3. ε dependence of $Z(t)$ [Eq. (A14)] for $\alpha = \beta = 10\gamma_1$. Curves from top: $\varepsilon = 1, 0.3, 0.1, 0.03, 0.01$.

ally are shown in Figs. A1–A3 for various values of ε, $\alpha a^2/D$, and $\beta a^2/D$. Obviously the long-time behaviour is dominated by the term with the slowest decaying exponential but its amplitude is affected by the other coefficients. When α or β is the smallest exponent, the plot looks like a simple exponential decay apart from the smooth turnover at short times. For fixed high α and β and a fixed lower γ_1 (diffusion dominated), the plots for different ε become parallel lines at long times, reflecting the negligible contribution of all but the most slowly decaying term ($k = 1$). The loss at short times increases as ε decreases. As ε increases, $\rho^*(r)$ becomes more peaked toward the center of the sphere and the weight G_1 becomes more predominant so that $n_P(t)$ and $N_V(t)$ become closer to a single exponential decay after the initial turnover. It should be possible to use the data in this initial region to estimate the other exponents which are negligible at long times, though this process may not be entirely unambiguous. When several of the exponents have close or equal values, special care must be taken in evaluation as noted above.

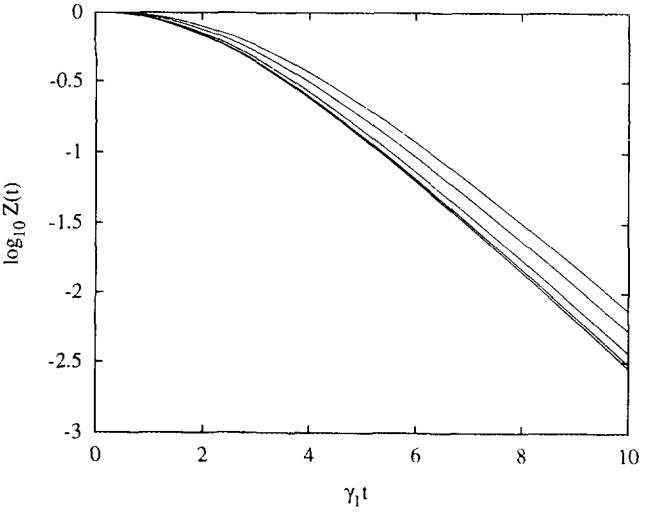

FIG. A2. ε dependence of $Z(t)$ [Eq. (A14)] for $\alpha = \beta = \gamma_1$. Curves from top: $\varepsilon = 1, 0.3, 0.1, 0.03, 0.01$.

ACKNOWLEDGMENTS

The authors thank BP Chemicals for permission to publish this work, and Dr. J. W. Couves and Dr. J. C. Frost for considerable technical assistance and many useful discussions.

REFERENCES

1. Leonard, E. C., "Vinyl and Diene Monomers: Part I," Chap. 5, pp. 263–319. Wiley-Interscience, New York, 1970.
2. Moiseev, I. I., Vargaftic, M. N., and Syrkin, Ya. K., *Dokl. Akad. Nauk. USSR* **133,** 377 (1960).
3. *Chem. Week* **101**(7), 73 (1967); British Patent Nos. 964001, 969162, 975709, 1026594, 1061788.
4. *Eur. Chem. News* **11**(272), 40 (1967); *Chem. Ind.*, 1559 (1968).
5. *World Pet. Cong. Proc* **5,** 41 (1968).
6. U.S. Patent No. 3658888 (1967).
7. U.S. Patent No. 4048096 (1977).
8. Biloen, P., Helle, J. N., van den Berg, F. G. A., and Sachtler, W. M. H., *J. Catal.* **81,** 450 (1983).
9. Mims, C. A., and McCandlish, L. E., *J. Phys. Chem.* **91,** 929 (1987).
10. Ekstrom, A., and Lapszewicz, J. A., *J. Phys. Chem.* **93,** 5230 (1989).
11. Janssen, F. J. J. G., van den Kerkhof, F. M. G., Bosch, H., and Ross, J. R. H., *J. Phys. Chem.* **91,** 5921 (1987).
12. Renken, A., Doepper, M., and Schmid, M., "Study of Heterogeneous Catalytic Kinetics," Dechema-Monographs Vol. 120, p. 273. VCH Verlagsgesellschaft, Weinheim, 1989.
13. Nakamura, S., and Yasui, T., *J. Catal.* **17,** 366 (1970).
14. Nakamura, S., and Yasui, T., *J. Catal.* **23,** 315 (1971).
15. Zaidi, S. A. H., *Appl. Catal.* **38,** 353 (1988).

16. Samanos, B., Boutry, P., and Montarnal, R., *J. Catal.* **23,** 19 (1971).
17. Winston, S., *J. Am. Chem. Soc.* **98,** 6914 (1976).
18. Maitlis, P. M., "The Organic Chemistry of Palladium." Vol II: "Catalytic Reactions." Academic Press, New York, 1971.
19. Bryant, D. R., and McKeon, J. E., "Symposium on Homogeneous Catalytic Reactions Involving Palladium." *ACS Div. Pet. Chem.* **14**(2), Preprint B1A (1969).
20. Davidson, J. M., Mitchell, P. M., and Raghavan, N. S., *Front. Chem. React. Eng.* [*Proc. Int. Chem. React. Eng. Conf.*] **1,** 300 (1984).